Multistage Infrared Emitters Based on InAsSb Strained Layers Grown by Metal-Organic Chemical Vapor Deposition

R. M. Biefeld, A. A. Allerman, S. R. Kurtz, and K. C. Baucom
Sandia National Laboratory, Albuquerque, New Mexico, 87185-0601, USA

Abstract - **We report on the metal-organic chemical vapor deposition (MOCVD) of mid-infrared InAsSb multistage emitters using a high speed rotating disk reactor. The devices contain AlAsSb claddings and strained InAsSb active regions. These emitters have multistage, type I, InAsSb/InAsP quantum well active regions. A semi-metal GaAsSb/InAs layer acts as an internal electron source for the multistage injection lasers and AlAsSb is the electron confinement layer. These structures are the first MOCVD multistage devices. Broadband LED's produced 2 mW average power at 3.7 μm and 80 K and 0.1 mW at 4.3 μm and 300K. A multistage, 3.8-3.9 μm laser structure operated up to T=180 K. At 80 K, peak-power > 100 mW/facet and a high slope-efficiency (48%) were observed in these gain guided lasers.**

I. Introduction

Mid-infrared (3-6 μm) lasers and LEDs are being developed for use in chemical sensor systems and infrared countermeasure technologies. These applications require relatively high power, mid-infrared lasers and LEDs operating near room temperature. The radiative performance of mid-infrared emitters has been limited by nonradiative recombination processes (usually Auger recombination) in narrow bandgap semiconductors. Potentially, Auger recombination can be suppressed in "band-structure engineered", strained, Sb-based heterostructures. We have demonstrated improved performance for midwave infrared emitters in strained InAsSb heterostructures due to their unique optoelectronic properties that are beneficial to the performance of these devices [1-3]. We are exploring the growth by metal-organic chemical vapor deposition (MOCVD) of novel, multistage (or "cascaded") active regions in InAsSb-based devices, to further improve laser and LED performance [4]. Multistage, mid-infrared gain regions have been proposed for several material systems [1-7]. Ideally, a laser with an N-stage active region could produce N photons for each injected carrier. Multistaging of the laser active region may increase gain, lower threshold current, and finally increase the operating temperature of gain-limited, mid-infrared lasers. The success of the unipolar, quantum cascade laser demonstrates the benefit of multistage gain regions [7]. Gain regions with multiple electron-hole recombination stages have been proposed for Sb-based lasers [1,5,6]. Recently, cascaded lasers with type II InAs/GaInSb active regions have been demonstrated [8]. These type II lasers were grown by molecular beam epitaxy, and, characteristic of multistage lasers, differential quantum efficiencies exceeding one are now reported [9]. In this paper we report on our 10-stage lasers with InAsSb/InAsP quantum wells and type I band offsets with differential quantum efficiencies exceeding unity.

A band diagram of a single stage in our multistage active region, under forward bias, is shown in Figure 1. Electron-hole recombination occurs in compressively strained InAsSb quantum wells separated by tensile strained InAsP barriers. Electron-hole pairs for each stage are generated at a semi-metal, GaAsSb (p)/ InAs (n) heterojunction. An AlAsSb layer prevents electrons from escaping; nominal hole confinement is provided by the InAsSb quantum well valence band offset relative to the InAsP barrier layer in this initial device. Ideally, electron-hole generation replenishes the carriers which recombine in each stage, and for each carrier injected from the external circuit, the multistage active region can emit several photons resulting in an overall quantum efficiency greater than unity. Previously, we have found that an AlGaAsSb graded layer between the AlAsSb and GaAsSb layers reduces hole trapping, thus increasing laser duty cycles and lowering turn-on voltages [4]. We have observed similar improvements in devices containing either a heavily doped GaAsSb/AlAsSb interface or a GaAsSb/AlAsSb short period superlattice.

Unlike previous cascaded lasers and LEDs [5-9] our device was grown by MOCVD [4]. Our devices are among the most complex structures ever grown by MOCVD, and it can be difficult to alternate Al, In, Ga, P, As, or Sb bearing materials while maintaining sharp interfaces and managing chemical carry-over into other layers. We have found that the combination of novel Al organometallic sources and an MOCVD, vertical, high speed rotating-disk reactor (RDR) are necessary to grow these structures to avoid the chemical carry-over previously observed with a horizontal reactor [3]. Even with an RDR, it is necessary to optimize the growth conditions and the reactor configuration as discussed below to minimize the possibility of chemical carry over.

II. Experimental

This work was carried out in a previously described vertical, high-speed, rotating-disk reactor (RDR) [10]. Ethyldimethylamine alane (EDMAA), trimethylindium (TMIn), triethylgallium (TEGa), triethylantimony (TESb), diethylzinc (DEZn), phosphine, and tertiarybutylarsine

DISCLAIMER

DISCLAIMER

Portions of this document may be illegible in electronic image products. Images are produced from the best available original document.

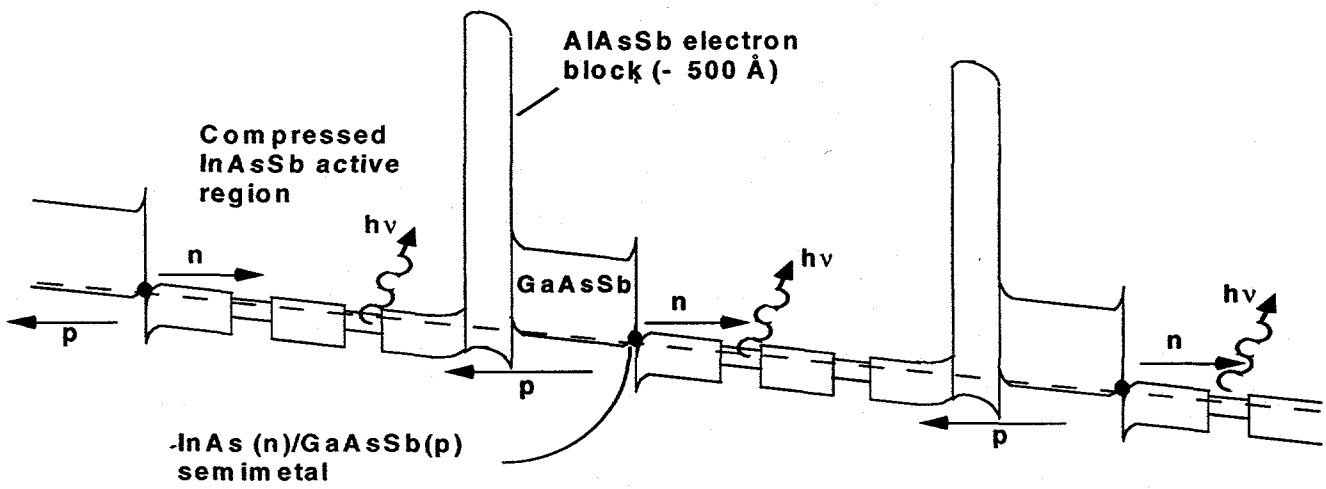

Fig. 1. Band diagram of a multistage laser active region with compressed, type I InAsSb quantum wells separated by InAsP barriers, electron-hole generation by an InAs(n)/GaAsSb(p) semi-metal heterojunction, and an AlAsSb electron block.

(TBAs) or arsine were used as sources. P-type doping was accomplished using diethylzinc (DEZn) in a dilution system. The structures were grown at 500 °C and 70 torr. The V/III ratios were optimized separately for each material and the InAsSb/InAsP strained-layer superlattice. Hydrogen was used as the carrier gas at a flow of 18.5 slpm with a substrate rotation speed of 1500 rpm to retain matched flow conditions [10]. Semi-insulating, epi-ready (001) GaAs for Hall samples or n-type (001) InAs substrates were used for each growth.

Both InAsSb/InAs and InAsP/InAs multiple quantum wells (MQWs) were grown for calibration purposes to determine the solid-vapor distribution coefficients separately for Sb in InAsSb and P in InAsP. The InAsSb/InAsP SLSs were lattice matched to InAs with a mismatch of less than 0.0004. The MQW and SLS composition, layer thickness, and strain were determined by double crystal x-ray diffraction (DCXRD). DCXRD was also used to determine alloy composition. Alloy layer thicknesses were determined using a groove technique and these were checked in several instances by cross sectional SEM. These techniques agreed to within a few percent.

Infrared photoluminescence (PL) was measured on all samples at 14 K and 300 K using a double-modulation, Fourier-transform infrared (FTIR) technique. This technique provides high sensitivity, reduces sample heating, and eliminates the blackbody background from infrared emission spectra. Injection devices also were characterized with double modulation FTIR.

III. Results and Discussion

1.MOCVD Growth

The best growth conditions found in this investigation for $AlAs_xSb_{1-x}$ occurred at 500 °C and 70 torr at a growth rate of 3.2 Å/s using a V/III ratio of 5.3. The V/III ratio was calculated using a vapor pressure of 0.75 torr for EDMAA at 19.8 °C and an [TESb]/([TBAs]+[TESb]) ratio of 0.83. The growth rate was found to be dependent on the EDMAA flow and independent of the group V flows for the conditions examined in this work. The best surface morphologies with the lowest number of defects were obtained by using a buffer layer grown before the $AlAs_xSb_{1-x}$ layer. The defects consisted primarily of square pyramidal hillocks 10 to 20 μm on a side. Lattice matched $AlAs_xSb_{1-x}$ films of high crystalline quality, as evidenced by DCXRD where full widths at half of the maximum intensity (FWHM) of 27 to 50 arc seconds were obtained. Typical InAs substrate peaks were 10-20 arc seconds. The x-ray peak width of 50 arc seconds could be due to some variation in composition with growth time as discussed below or to phase separation. We were also able to reproducibly obtain lattice matching of $AlAs_xSb_{1-x}$ to InAs to within less than 0.00015 using the optimized growth conditions. Hall measurements of AlAsSb films 1 μm thick with 200Å GaAsSb cap layers grown on GaAs substrates indicated background hole concentrations between 0.5 to 1 $x10^{17}$ cm^{-3}. The residual hole concentration of GaAsSb films on GaAs ranged between 4 to $7x10^{16}$ cm^{-3}. The use of other than the above stated growth conditions led to several significant problems during the growth of

$AlAs_xSb_{1-x}$ layers lattice matched to InAs. These included composition control and reproducibility. For instance, growth at higher V/III ratios resulted in a large drift in composition from run to run and broad x-ray diffraction peaks. Composition variations have also been observed due to excess cooling of the chamber walls which resulted in an Sb memory effect on the inlet to the reactor.

We have successfully doped the $AlAs_xSb_{1-x}$ layers p-type using DEZn. We achieved p-type levels of 1 x 10^{16} to 6 x 10^{17} cm^{-3}. The mobilities for the $AlAs_xSb_{1-x}$ layers ranged from 200 to 50 cm^2/Vs with no clear trend that could be associated with the carrier concentration. The Zn doping levels were determined from Van der Pauw/Hall measurements and confirmed by secondary ion mass spectroscopy (SIMS) on thick calibration samples. SIMS measurements on the Zn doped samples indicated a similar level of Zn compared to the p-type carriers indicating complete activation of the Zn. Two orders of magnitude higher DEZn partial pressures were required to obtain equivalent dopant levels in $AlAs_{0.16}Sb_{0.84}$ compared to $GaAs_{0.09}Sb_{0.91}$. This lower incorporation rate for Zn in AlAsSb indicates a possible depletion reaction between DEZn and EDMAA.

Growth rates of 2.8 Å/s were used for the growth of InAsSb/InAs and InAsP/InAs MQW structures. The growth rate was found to be proportional to the TMIn flow into the reaction chamber and independent of the group V flows. A purge time of 15 to 20 seconds with arsine flowing during the purge was used between InAs and the ternary layer growth to allow for source flow changes during the growth of the MQWs. For the InAsSb layers, the V/III ratio varied from 1.9 to 5.9. The composition was changed by varying the TBAs flow. A low V/III ratio is necessary for the growth of high quality InAsSb due to the low vapor pressure of Sb; excess Sb tends to cause surface morphology defects. For InAsP the V/III ratio is dominated by the excess phosphine flow and was approximately constant at 70. The high V/III ratio and excess phosphine flow are necessary because of the high decomposition temperature of phosphine. The composition of InAsP was adjusted by varying the TBAs flow. In both cases, InAsSb/InAs and InAsP/InAs, the composition dependence was reproducible and approximately linear over the composition range that was examined.

Several test laser structures were prepared similar to the one previously reported using InAsSb/InAs MQW active regions [3]. These structures consisted of 2 μm p-type AlAsSb top and bottom cladding layers with InAsSb/InAs 10 period MQW active regions and a (p)-GaAsSb/(n)-InAs semi-metal heterojunction for charge transfer [1-3]. There was a marked improvement in the quality of the x-ray diffraction pattern of the continuously grown structure from the RDR and that of the re-grown active region and top cladding from the horizontal system. Similar lasing characteristics were obtained for both the RDR and re-grown structures. The advantage of the RDR growths is that no Al carry-over was

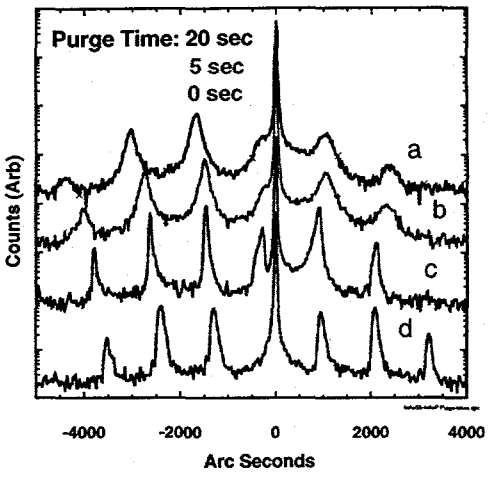

Figure 2. Comparison of the x-ray diffraction patterns for InAsSb/InAsP SLS's grown using identical growth conditions in (a), (b), and (c) but with the indicated purges between layers [(a) = 20 sec., (b) = 5 sec., and (c) = 0 sec.]. The sample in (d) was grown with a slightly different composition than (c) with no purge time to achieve lattice matching with the InAs substrate.

observed as was found for the structures grown using the horizontal reactor without re-growth [3]. The multistaged laser structures described in this paper would be impractical to grow using the re-growth technique developed in our conventional horizontal MOCVD system.

The growth of the InAsSb/InAsP ternary strained-layer superlattices (SLSs) used similar conditions as those for the MQW growths. The growth conditions for a given composition of the SLS was easily predicted from the compositions of the MQW's. However, very rough surface morphologies and poor x-ray diffraction patterns and photoluminescence characteristics were found for the 15-20 second purge times used between layers. The purge times were optimized using both x-ray diffraction patterns, as illustrated in Figure 2, as well as photoluminescence. As shown in Figure 2(a) and (b) for purge times of 20 and 5 seconds, very broad x-ray diffraction patterns were observed. The x-ray diffraction patterns shown in Figure 2(c) and (d) differ only in composition; both were grown using no purges between layers. The sample in (d) was grown with a slightly different composition to achieve lattice matching with the InAs substrate. Similar characteristics were found for purge times of 0 or 1 second with arsine continuing to flow during the purge times as well as during the growth of the layers.

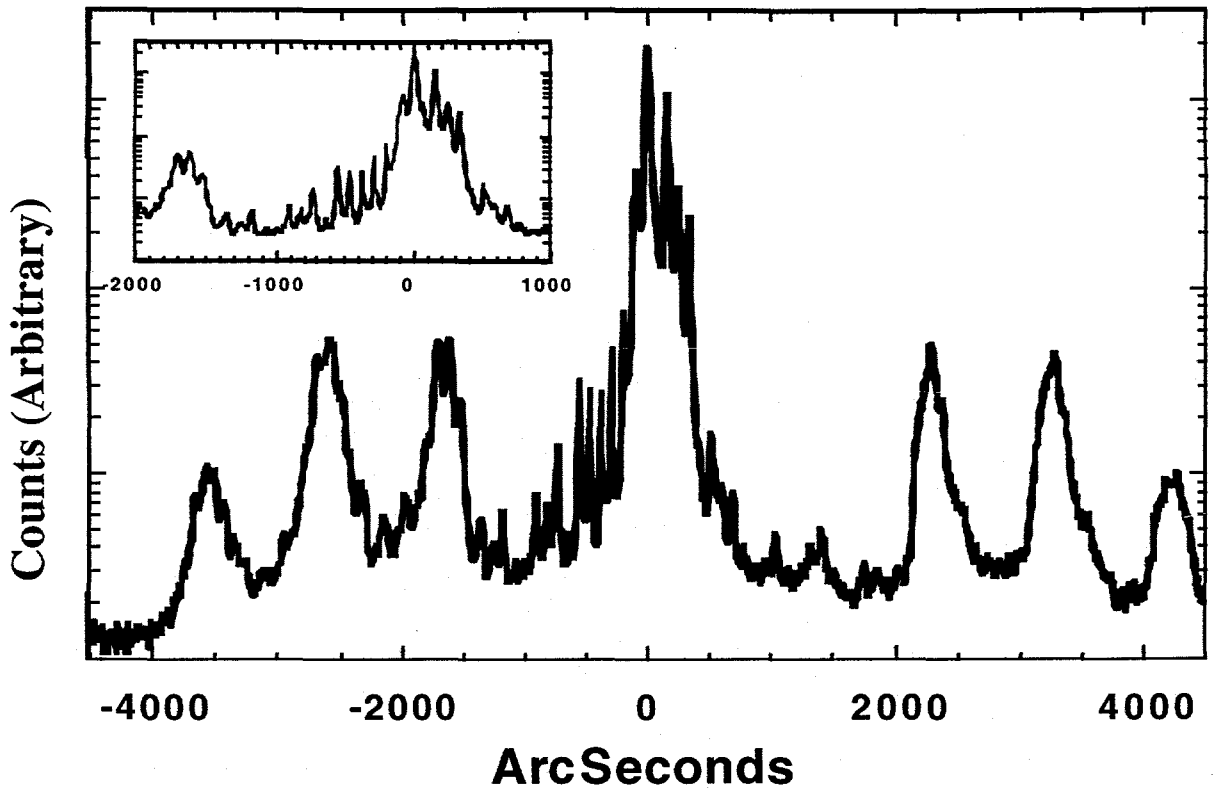

Figure 3. X-ray diffraction pattern for a 10-stage, 5-well InAsSb/InAsP laser structure with 2 μm AlAsSb claddings and p-GaAsSb/n-InAs semi-metal heterojunction injection layers.

2. Ten-Stage, Cascaded InAsSb Quantum Well LEDs and Lasers at 3.9 μm

We have prepared ten-stage, cascaded InAsSb quantum well lasers. Each stage consisted of a $GaAs_{0.09}Sb_{0.91}$ (p, 300 Å) /InAs (n, 500 Å) semi-metal , 3 or 5 $InAs_{0.85}Sb_{0.15}$ (n, 94 Å) quantum wells separated by 4 $InAs_{0.67}P_{0.33}$ (n, 95 Å) barriers, an $AlAs_{0.16}Sb_{0.84}$ (p, 50 Å) electron block, a compositionally graded, Zn-doped AlGaAsSb (p = 5×10^{17} cm^{-3}, 300 Å) layer and a final 50 Å, Zn-doped $GaAs_{0.09}Sb_{0.91}$ layer. The total thickness of the gain region is 1.9 μm. The excellent crystalline quality of these laser structures is demonstrated in the x-ray diffraction spectrum of the 5 well active region where groups of satellite peaks corresponding to a gain-stage period of 2100 Å and the InAsSb/InAsP period of 190 Å are observed as illustrated in Figure 3. The composition and layer thickness for the InAsSb/InAsP superlattice can be determined from the satellites with the large repeat distance where the smaller repeat distance as shown in the inset is determined by the 10-stage structure.

Optical confinement for these lasers is provided by 2 μm thick , Zn-doped $AlAs_{0.16}Sb_{0.84}$ ($p=1 \times 10^{17} cm^{-3}$) claddings on both sides of the active region. A top 1500 Å Zn-doped $GaAs_{0.09}Sb_{0.91}$ layer ($p=2 \times 10^{18}$ cm^{-3}) is used as a contact and protective layer. The structure is lattice matched to the InAs substrate. An InAs (n, 500 Å) /$GaAs_{0.09}Sb_{0.91}$ (p, 1000 Å) semi-metal is used to enable carrier transport from the n-type InAs substrate into the p-type $AlAs_{0.16}Sb_{0.84}$ cladding layer.

Narrow LED and photoluminescence emission peaks of the 10-stage laser wafers indicated good stage-to-stage uniformity of the InAsSb/InAsP multiple quantum wells (see Figures 4 and 5). Only InAsSb/InAsP emission was observed in the LED spectrum. Emission from the InAs layer would be a strong indication of inadequate carrier confinement in the InAsSb quantum wells. The LED emission wavelength shifted from 3.7 μm (80 K) to 4.3 μm (300 K) due to the temperature dependence of the InAsSb/InAsP bandgap. Operated at 50% duty cycle, average LED output powers were 2.4 mW at 80 K and 100 μW at 300 K when driven with 200 mA average current. We speculate that the rapid decrease in LED power with temperature is due to thermal emission of holes from the InAsSb/InAsP quantum wells.

Lasing was observed from gain-guided stripe lasers. The facets were uncoated, and stripes were indium soldered to the heat sink with the epitaxial side up. Under pulsed operation with 100 nsec pulses at 1 kHz (10^{-4} duty-cycle), stimulated emission was observed from 80-180 K and 3.8 to 3.9 μm. Laser emission spectra at 80 K and 150 K are shown in Figure 5. For 500 μm long stripes with 80 μm wide

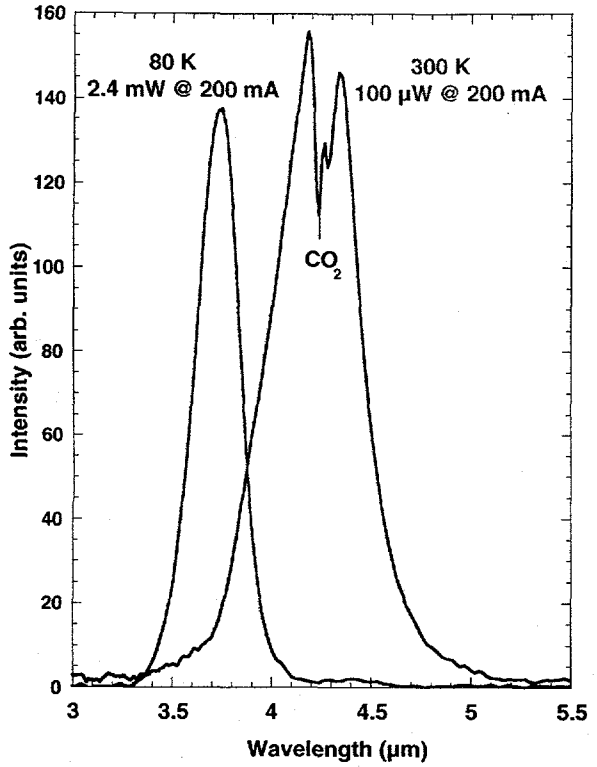

Fibgure 4. The LED emission peaks of a ten-stage InAsSb/InAsP multiple quantum well laser structure.

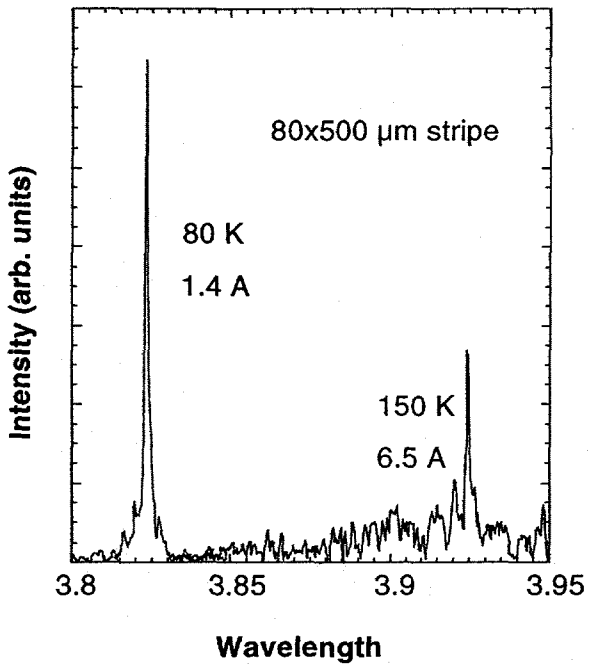

Firure 5. Emission spectra at 80 K and 150 K for a ten-stage, five well, cascaded, InAsSb laser structure with a 500 µm stripe.

metallizations, several longitudinal modes are observed with a mode spacing of 2.7 cm^{-1}. The longest laser pulses were 1 µsec. These initial devices were easily damaged by increased heating associated with higher temperature operation or longer duty cycles. Threshold current densities for these 10-stage devices were = 1 kA/cm^2. Lower threshold current densities (0.1 kA/cm^2) have been demonstrated in single-stage, type I mid-infrared lasers at 80 K [12]. The temperature dependence of the threshold current is shown in Figure 6 for an 80x250 µm, 10-stage laser. The T_0 of the 5-well laser was 34 K which is similar to our previously reported, optically pumped and injection InAsSb/InAsP lasers [2].

The laser output was collected and focused directly onto an InSb detector to obtain power-current data. At 80 K, peak power values > 100 mW/facet were obtained. The maximum slope-efficiency was 150 mW/A, corresponding to a differential external quantum efficiency of 48 % (4.8 % per stage). This initial result is promising when compared to the value obtained for a second generation, 23-stage type II cascaded laser (3.9 µm) with a differential quantum efficiency of 131% (5.7 % per stage) [4].

Multistage laser slope-efficiency (or differential-efficiency) was strongly dependent on cavity length [4].

Power-current curves for 10-stage laser stripes with lengths of 250-1000 µm are shown in Fig. 7. These results are plotted as $(\text{differential-efficiency})^{-1}$ versus cavity length in Fig. 8. Scatter in the data prevents accurate determination of internal efficiency and loss coefficient, but the best fits are obtained for internal efficiency values in the range 1-10, strongly suggesting an internal quantum efficiency > 1. Depending on this internal efficiency value, we obtain a loss coefficient $\geq$ 100 cm^{-1} for our devices. Large losses may be caused by intersubband absorption of the InAsSb/InAsP quantum wells or free carrier absorption in semimetal layers or heavily doped cladding and heterobarrier layers. Comparison of absorption spectra for single-stage and 10-stage laser wafers reveals absorption of the correct magnitude associated with the 10-stage gain region, suggesting that the loss originates from the semimetal design or doping in the active region. A lower sheet carrier density can be achieved with quantum confinement of the semimetal, like that used in type II cascade laser designs [9]. We doubt that absorption in the InAsSb quantum wells is causing the loss because such high loss has not been observed in other type I, Sb-based lasers. Reduction of loss will be a major hurdle in the advancement of Sb-based, injection lasers, especially cascaded devices.

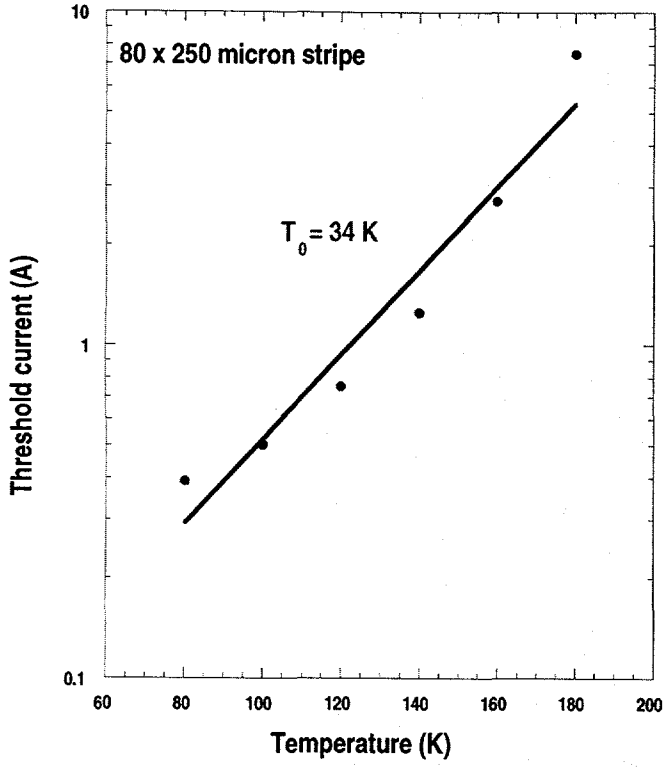

Fig. 6. The temperature dependence of the threshold current for an 80x250 μm, ten-stage laser.

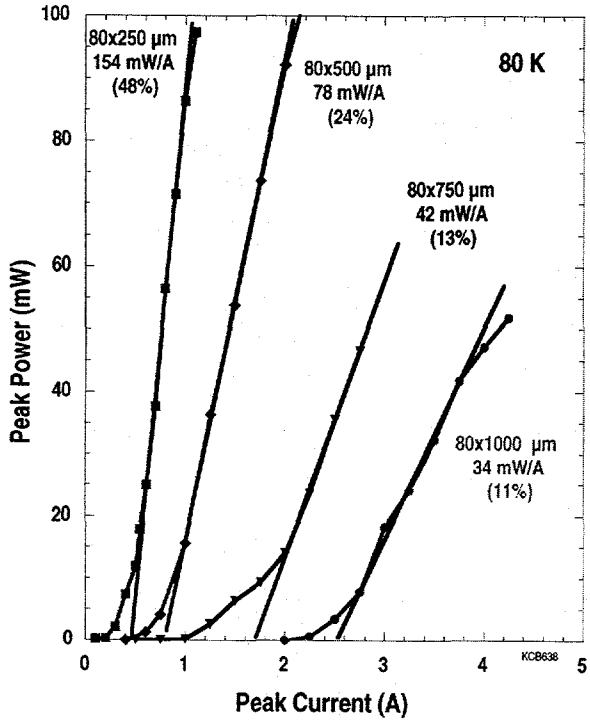

Fig.. 7. Power-current curves and slope efficiencies for 250, 500, 750, and 1000 μm long laser stripes at 80 K.

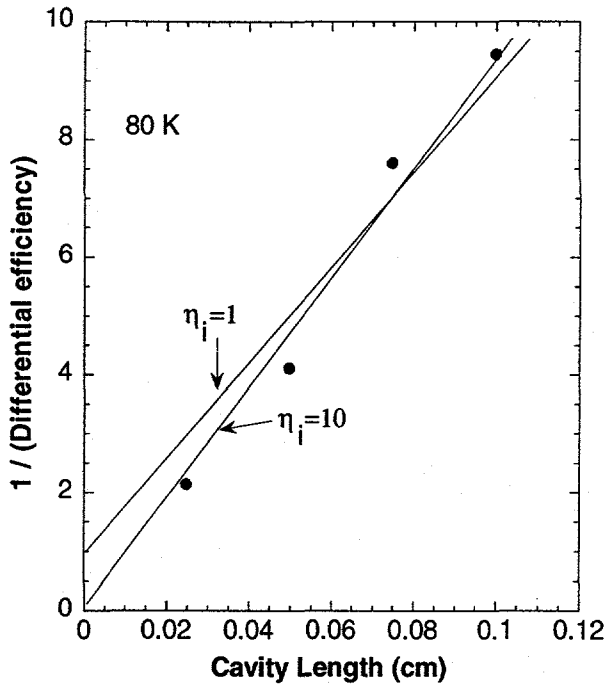

Fig. 8. Plot of 1/(slope efficiency) vs. cavity length data as shown in Fig. 7. Lines corresponding to internal differential efficiencies (η_i) of 1 and 10 are shown.

IV. Summary

In conclusion, we have demonstrated the first cascaded lasers and LEDs with type I InAsSb quantum well active regions grown using MOCVD. Also, these are the first cascaded devices grown by MOCVD. The 10-stage, 3.8-3.9 μm laser operated up to 180 K. At 80 K, peak laser power > 100 mW/facet and a slope-efficiency of 48% (4.8% per stage) were observed with internal quantum efficiencies > 1. We are optimistic that advances in material quality and device design will improve carrier confinement and reduce loss, leading to higher efficiencies and higher temperature operation of cascaded InAsSb lasers.

ACKNOWLEDGMENTS

We thank J. A. Bur for technical assistance. This work was supported by the U.S. Dept. of Energy under contract No. DE-AC04-94AL85000. Sandia is a multiprogram laboratory operated by Sandia Corporation for the United States Department of Energy.

References

[1] A. A. Allerman, R. M. Biefeld, and S. R. Kurtz, "InAsSb-based mid-infrared lasers (3.8-3.9 μm) and light-emitting

diodes with AlAsSb claddings and semi-metal electron injection grown by metal-organic chemical vapor deposition," Appl. Phys. Lett. vol. 69, pp. 465-467, 1996.
[2] S. R. Kurtz, A. A. Allerman, and R. M. Biefeld, "Midinfrared lasers and light-emitting diodes with InAsSb/InAsP strained-layer superlattice active regions" Appl. Phys. Lett. vol. 70, pp. 3188-3190, 1997.
[3] R. M. Biefeld, S. R. Kurtz, and A. A. Allerman, "The metalorganic chemical vapor deposition growth of AlAsSb and InAsSb/InAs using novel source materials for infrared emitters," J. Electronic Mater., vol. 26, pp. 903-909, 1997.
[4] S. R. Kurtz, A. A. Allerman, R. M. Biefeld, and K. C. Baucom, "High slope efficiency, "cascaded" midinfrared lasers with type I InAsSb quantum wells," Appl. Phys. Lett. vol. 72, pp. 2093-2095, 1998.
[5] C. L. Felix, W. W. Bewley, I. H. Aifer, I Vurgaftman, J. R. Meyer, C. H. Lin, D. Zhang, S. J. Murry, S. Q. Yang, and S. S. Pei, "Low Threshold 3 mm interband cascade "W" laser," J. Electron. Mater. vol. 27, pp. 77-80, 1998.
[6] J. R. Meyer, I. Vurgaftman, R. Q. Yang, and L. R. Ram-Mohan, "Type II and type I interband cascade lasers," Elect. Lett. vol. 32, 45-46, 1996.
[7] J. Faist, F. Capasso, C. Sirtori, D. L. Sivco, J. N. Baillargeon, A. L. Hutchinson, S. N. G. Chung, and A. Y. Cho, Appl. Phys. Lett., "High power mid-infrared (≈5μm) quantum cascade lasers operating above room temperature," 68, pp. 3680-3682, 1996, and references therein.
[8] C. H. Lin, R. Q. Yang, D. Zhang, S. J. Murry, S. S. Pei, A. A. Allerman, and S. R. Kurtz, "Quantum cascade light emitting diodes based on type-II quantum wells," Elect. Lett. vol. 33, pp. 598-599, 1997.
[9] R. Q. Yang, B. H. Yang, D. Zhang, C. H. Lin, S. J. Murry, H. Wu, and S. S. Pei, "High power midinfrared interband cascade lasers based on type II quantum wells," Appl. Phys. Lett. 71, 2409-2411, 1997.
[10] W. G. Breiland and G. H. Evans, "Design and verification of nearly ideal flow and heat transfer in a rotating disk chemical vapor deposition reactor," J. Electrochem. Soc., vol. 138, pp. 1806-1816, 1991.
[11] H.K. Choi and G.W. Turner, "InAsSb/InAlAsSb strained quantum-well diode lasers emitting at 3.9 μm,"Appl. Phys. Lett. 67, 332-334, 1995.